

is experimentally more demanding. One suitable method is inverse photoemission spectroscopy (IPES). As the name implies, this is the reversed process of photoelectron emission: Electrons are shot on the sample and may be captured in unoccupied states [slide]. This is the an excited, metastable state of the system which can decay to a state closer to  $E_{\text{kin}}$  by emission of a photon. The conservation of energy in this case is written as:

$$\hbar\omega = E_{\text{kin}} + \epsilon f + E_b$$

Note that the binding energy of an unoccupied state is negative. IPES faces several experimental difficulties. First, the cross section of the process is low. Second, it is much more difficult to detect energy-resolved photons than electrons.

A second method is two-photon photoemission (T2PPE) [slide]. Here, an electron is excited into a state below the vacuum level. From this metastable state it can decay to a state with lower energy on the timescale of femtoseconds. When it is hit by another photon before this decay, it can be transferred above the vacuum level and detected. To achieve this, high photon-fluxes are necessary. Consequently, lasers are used. By putting in a delay between the two pulses, the dynamics of the excited state can be explored (lifetime). This is called a pump-probe experiment.

## X-ray absorption spectroscopy (XAS)

Up to now, we only looked at the photoelectrons excited by the x-ray photons. However, much can also be learned by looking at the absorption of the x-rays itself. The basis is again the photoelectric effect. We already know that an x-ray can only be adsorbed by an atom when its energy is greater than or equal to the binding energy of an electron. We have already introduced the law of Lambert-Beer, which reads:

$$I = I_0 e^{-\mu t} \quad \begin{matrix} \text{incident intensity} \\ \rightarrow \\ \text{transmitted intensity} \end{matrix} \quad \begin{matrix} \text{thickness} \\ \leftarrow \text{absorption coefficient} \end{matrix}$$

At most x-ray energies, the absorption coefficient  $\mu$  is a smooth function of energy and can be written as:

$$\mu \approx \frac{S Z^4}{A E^3} \quad \begin{matrix} \text{density} \downarrow & \text{atomic number} \swarrow \\ \text{atomic mass} & \rightarrow \text{x-ray energy} \end{matrix}$$

Looking at real curves of  $\mu(E)$  reveals a more complex behaviour [slide]. When the incident x-ray has an energy equal to that of the binding energy of a core electron, there is a sharp rise in absorption: an absorption edge corresponding to the promotion of this core electron to the continuum. For some reasons, the edges belonging to  $n=1, 2, 3\dots$  are named K, L, M.

In X-ray absorption fine structure (XAFS), one looks at  $\mu(E)$  near and at energies just above these absorption edges.

In order to detect the absorption of the photon, one looks at the decay of the associated excited state of the atom. There are two basic processes at work here. The first one is X-ray fluorescence [slide] in which a higher energy core-level electron fills the deeper core-hole, ejecting an X-ray of well-defined energy (to conserve energy). The fluorescence energies emitted in this way are characteristic of the atom and can be used to identify the atoms in a system and to quantify their concentrations. The second process for de-excitation is the Auger-effect, in which an electron drops from a high level and now transfers its energy to a third electron which is emitted from the atom. Although this might seem a rather complicated process, for lower energy X-ray absorption ( $< 2 \text{ keV}$ ) it is actually the dominating one. Experimentally there are different methods to measure the absorption [slide]. First, rather straight forward, determine the beam intensity before and after the sample (transmission mode). Second, record the fluorescence (fluorescence yield). Third, measure all electrons that leave the sample by recording the current needed to refill electrons (total yield). Finally, record the photoelectrons above a certain threshold (partial yield). - (52)

As an example, the [slide] shows a typical XAFS spectrum for FeO. Depending on how close to the edge you look, the technique is further divided into X-ray absorption near-edge spectroscopy (XANES) and extended XAFS (EXAFS). The sharp rise in  $\mu(E)$  due to the Fe 1s electron level (at 7112 eV) is clearly visible in the spectra, as are the oscillations in  $\mu(E)$  that are the XAFS. Let us first look at the oscillations in the EXAFS-regime.

They are caused by interference effects between neighboring atoms: The excited electron is scattered at the neighboring atoms which leads to accumulation or depletion of charge density, which in turn influences the absorption probability of the photon. By going through the full theory, the number, distance, and chemical species of the neighbors can be determined. Very close to the edge (XANES-regime), the excited electron is not always brought to an energy above the vacuum level, but resides in metastable states close to it. This enhances the probability of absorption. In consequence, one can derive information on the chemical environment from this part of the spectrum. By using polarized light, one can also learn something about the direction of chemical bonds.

## Synchrotron light sources

Already several times during this lecture, we looked at experiments performed at synchrotron light sources (X-ray diffraction, X-ray photoelectron spectroscopy). This chapter now introduces this experimental method in more detail. The main characteristics of synchrotron radiation are:

- extremely high intensity (brilliance)
- broad energy range
- very good collimation
- polarization
- pulsed emission.

In short, a tunable light source with fantastic properties!

The principle of light generation is photon emission from accelerated charges, where the most simple example is the dipole antenna [slide]. A charge oscillating on a straight wire induces electromagnetic radiation. The maximum intensity occurs perpendicular to the acceleration of the charge. This general effect does also occur for a charge on a circular orbit (constant acceleration towards the center of orbit).

[slide] In a synchrotron, electrons with a speed close to the speed of light are used, which makes a relativistic description necessary. Basically, the high energy electrons emit very intense radiation, focused in a sharp forward cone.

The generation of synchrotron radiation is occurs in four steps [slide]. Electric fields are used to accelerate the electrons, and magnetic fields are used to define the electron path. First, electrons are created in an electron gun. In the next step, the electrons are accelerated in a linear accelerator. The main part is the booster synchrotron where the electrons go up to their final energies. In this ring-shape device, the electrons pass the accelerating E-field many times. To keep them on the desired orbit, the magnetic field has to be ramped up in synchronicity with the increase in energy (hence synchrotron). Finally, the electrons are transferred to the storage ring, where their velocity is constant. The energy loss due to emission of radiation is compensated by fields. The emitted light is extracted from the ring to a large number of beamlines.

Historically, however, the interest in synchrotrons came from particle physics where high energy particles were needed for collision experiments. In this context, synchrotron radiation was an undesired side effect as it leads to loss of energy. Solid state physicist, however, realized the high potential of synchrotron radiation and started to build beamlines at facilities focused on particle physics (parasitic use).

This changed when the first machines specifically designed to produce synchrotron radiation were put into use (~ 1980s), the second generation synchrotrons. During the use of the machines devices specifically designed for the excitation of synchrotron light were invented, the wiggler and the undulator (called insertion devices)

Synchrotrons especially designed to incorporate a large number of insertion devices form the third generation [slide] Let us now look at bending magnets, wiggles, and undulators in more detail.

Due to the relativistic behavior of the electrons, the cone of the emitted light is very narrow [slide] Consequently, one electron gives out a very short pulse of light for an observer sitting tangentially to the storage ring. The frequency (energy) spectrum is therefore very broad (it is the Fourier transform of the time domain) and contains rather high frequencies [slide]. Before we proceed, it is important to mention that several quantities can be used to describe synchrotron radiation:

$$\text{Total flux} = \frac{\text{Photons}}{\text{time}}$$

$$\text{Spectral flux} = \frac{\text{Total flux}}{0.1\% \text{ bandwidth}}$$

$$\text{Brightness} = \frac{\text{Total flux}}{\text{Solid angle} \cdot 0.1\% \text{ bandwidth}}$$

$$\text{Brilliance} = \frac{\text{Total flux}}{\text{Solid angle} \cdot \text{Source area} \cdot 0.1\% \text{ bandwidth}} \quad (56)$$

The brilliance is the figure of merit for third generation synchrotron. High total flux and small solid angle give a lot of photons on your sample, a lot of photons per wavelength interval allows you to select a highly monochromatized beam, and a small source ensures a high spatial coherence, useful for diffraction studies. The next [slide] shows the brightness normalized to the electron current for big magnets used for electrons of different energies and compares the flux with other sources.

For the insertion devices, the principle is to introduce alternating magnetic fields to the straight sections of the storage ring [slide]. Here, the electrons perform a wiggling or undulating motion, always emitting photons where the trajectory is curved [slide]. The special property of undulators is that the ones resulting from neighboring oscillation periods overlap and constructive interference occurs, resulting in a line spectrum of emission [slide]. The period of the magnets can be varied mechanically, thus allowing the use of different wavelengths.

The next [slides] compare the different devices and show the historical evolution of brightness.

### X-ray optics

In most of the cases, the generated radiation is not directly suitable for the experiment. It has to be monochromatized and focused [slide].

## Monochromator

For a monochromator, diffraction from a crystal is used [slide]. As we learned before, for a given angle only a specific wavelength will fulfill the diffraction condition. Even for the case of undulators, monochromators are still needed, as the bandwidth of the undulator is often too large and higher harmonics need to be suppressed. Very often, Si crystals are used, as the large, perfect crystals can be obtained and shaped. Using different planes, a wide range of energies can be covered [slide]. There are various designs in use with different properties, for example a double crystal monochromator where the beam does not move when the energy is changed. [slide]

## Mirrors

X-ray lenses cannot be easily build with high optical quality. Therefore, very often mirrors are used to focus the beam, based on Total reflection from surfaces below the critical angle [slide]. Focussing and collimation is then achieved by bending the magnet actively.

## Free electron laser

The most advanced light source available since a couple of years is the free electron laser (FEL). They provide unprecedented x-ray brightness ( $> 10^{10}$  times greater than in conventional synchrotrons) in pulses of very short duration. Short, intense pulses are especially needed in pump-probe experiments. [slide] A FEL does, for example, allow the probe to be x-ray diffraction. In such a machine, intensity can be high enough to record a diffraction pattern before the sample is destroyed by the beam. (diffact and destroy). The photons are obtained by accelerating a rather large number of electrons and then passing them through a long undulator. When the electrons start emitting photons, they still are travelling together with the electromagnetic field. This causes the electrons to bunch together so that later a large number of electrons will emit photons coherently, which again enhances the process (like in a laser). This is called spontaneous amplified self emission (SASE).

## Ultra-high vacuum technology

A lot of modern experimental in solid state physics request vacuum or even ultra-high vacuum (UHV). One reason is that only under UHV surfaces stay clean sufficiently long, the other reason is that electron beams (occurring in a lot of techniques) need vacuum to travel far enough.

Let us first look at the contamination of surfaces with adsorbing gases. From kinetic gas theory, one can calculate that the flux  $\Gamma$  of molecules impinging on a surface from the environment is given by:

$$\Gamma = \frac{P}{\sqrt{2\pi m k_B T}}$$

↑ pressure  
mass of ↑ temperature  
particle

This flux has to be compared to the areal density of atoms in the surface  $n_0$ . One often assumes that every atom or molecule impinging on a surface also sticks there and calls the number of particles needed to cover every surface atom with one gas atom a monolayer. The time constant to form a monolayer is then given as:

$$t = \frac{n_0}{\Gamma} = \frac{n_0 \sqrt{2\pi m k_B T}}{P}$$

From the ideal gas equation one knows:

$$PV = NK_B T$$

$$\Rightarrow n = \frac{N}{V} = \frac{P}{k_B T}$$

Finally, the mean free path of a particle is given as:

$$\lambda = \frac{k_B T}{\sqrt{2} \pi \sigma^2 P}$$

$\sigma$   
molecular  
cross section

To illustrate these quantities, let us look at  $N_2$  (main ingredient of air) at room temperature. For  $n_0$  we assume  $10^{19} \text{ m}^{-3}$  ( $\approx$  nearest neighbor distance on square lattice:  $3 \text{ \AA}$ ). For  $N_2$ , we assume a diameter of  $6 \text{ \AA}$ . The results are shown in the [slide]. Several things should now become clear:

- even at  $10^{-6} \text{ mbar}$ , a clean surface stays clean for roughly 1 s. For surface sensitive experiments, much lower pressures are therefore needed.
- in this pressure regime, the mean free path is usually much longer than the size of your machine. Therefore, for the individual gas atom, the vacuum seems perfect.
- Still, to us the particle classifying still appears very large.

In consequence, experiments where (i) the technique is intrinsically surface sensitive like PES or (ii) you are even particularly interested in surfaces, are performed under UNV condition ( $p \leq 10^{-10}$  mbar) [slide]

A second, somewhat weaker request for vacuum is the mean free path of electrons [slide].

Good vacuum conditions are needed in, e.g., a TEM. Due to the very long path of the electrons, a synchrotron needs UHV as well. Methods based on visible light, X-rays, or neutrons, as well as scanning probe microscopies, do not need vacuum.

Special pumps have to be used to reach UHV-conditions. The two most prominent are the Turbomolecular pump and the ion pump. The turbomolecular pump [slide] operates in the  $10^{-4}$  to  $10^{-11}$  mbar range and consequently a toughing pump is needed.

Basically, a turbo pump resembles a jet engine: a stack of rotors with multiple blades with angled leading edges is rotated at very high speed (50 000 to 100 000 rpm) and sweeps the gas molecules in the direction of the exhaust connected to the foreline. Turbo pumps are clean and reliable, but due to induced vibrations they are not suitable in systems with precise positioning, for example STM.

Ion pumps work in the  $10^{-3}$  mbar to  $10^{-11}$  mbar regime. [slide]. The basic configuration of an ion pump includes two plates made of Ti (cathode), mounted close to the open ends of short stainless steel tubes (anode), a strong magnetic field being applied parallel to the tube's axis. When an electron is situated inside the tube, the applied high voltage accelerates it towards the anode. The magnetic field forces them on a helical (and thus rather long) path. Collision of the electrons with gas molecules causes ionization. The gas ions are accelerated towards the cathode and are buried in the reactive Ti. At the same time, Ti is sputtered and coats the surfaces of the pump. Consequently, the reactive Ti binds additional gas atoms. The major advantages of ion pump are cleanliness, vibration free operation, and long operating life (no moving parts).

Special care has to be taken when selecting materials used in a UHV chamber.

A lot of materials have a vapor pressure, which is actually higher than the desired pressure inside your system [slide]. This includes almost all plastic or rubber materials, but also many metals. Today, all vacuum chambers are built out of steel and use copper gaskets [slide].

The base pressure that can be reached is given as:

$$P = \frac{L}{S_{eff}} .$$

Here,  $S_{eff}$  is the combined effective pumping speed of your pumps (measured in mbar l/s) and  $L$  is the leak rate. It consists of three parts: (i) real leaks, i.e. little openings to atmosphere, (ii) virtual leaks, i.e. small volumes of gas trapped in your chamber or brought in by unsuitable materials, and (iii) outgassing. Outgassing is due to the fact that under ambient conditions, all surfaces are fully covered by adsorbed gas (mostly water). In vacuum, this gas slowly desorbs. However, the amount of gas is so high and the desorption rate is so low that you can pump for months on a system and not reach UHV. The solution is to bake out your system, i.e. to raise the temperature to  $150 - 200^\circ$  for a few days in order to remove the adsorbed gas layer. Only thereafter the pressure will drop down to the  $10^{-10}$  mbar regime.

Also the determination of these low pressures needs special devices. The standard tool to determine pressures lower than  $10^{-3}$  mbar is the ionization gauge. (stick). Its operation is based on the ionization of molecules.

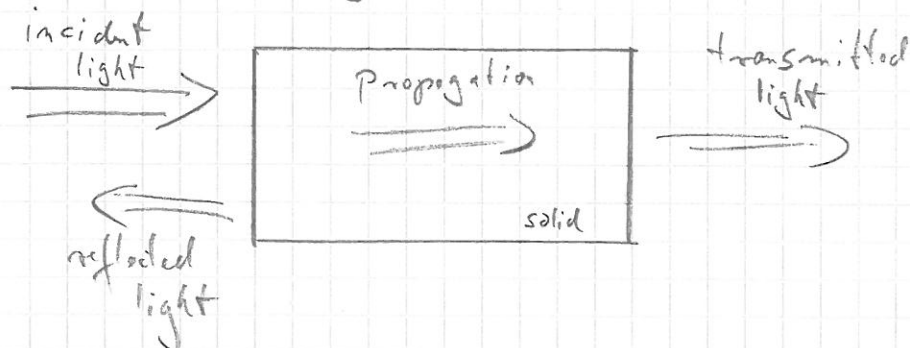
As the ionization rate and, hence, the ion current are directly dependent on the gas pressure, the pressure can be determined.

The Bayard-Alpert gauge depicted here uses electrons which are accelerated from a filament towards a grid which is at a higher potential than the filament. These electrons ionize atoms and molecules, which are then attracted towards the fine wire grounded collector situated at the center of the gauge. Finally, the collector current is converted to a pressure indication. The low pressure limit of the gauge arises mainly from the excitation of x-rays by the electrons bombarding the grid, which, in turn, excite disturbing photoelectrons. Ion gauge measurements are seriously affected by the gas composition.

Finally, there is a whole little industry supplying additional vacuum equipment, like valves, feed throughs for current or liquids, or devices enabling movement of parts inside the vacuum. A large UHV-system can quickly become quite complicated.

## Optical spectroscopy

The general phenomena that occur when light is shining on a solid can be grouped in reflection, propagation, and transmission:



During propagation, light can be refracted, absorbed, or scattered. Let us now describe these effect mathematically using the respective optical coefficients.

The reflection at surfaces is described by the coefficient of reflection or reflectivity  $R$ .

$R$  is defined as the ratio of reflected power to the power incident on the surface. The coefficient of transmission or transmissivity  $T$  is defined analogously as the ratio of transmitted power to incident power. If there is no absorption or scattering, then by conservation of energy we must have that:

$$R + T = 1$$

The propagation of light through a transparent medium is described by the refractive index  $n$ . It is defined as the ratio of the velocity of light in free space

$c$  to the velocity of light in medium ✓  
according to :  $n = \frac{c}{v}$

In general,  $n$  depends on the wavelength. When only a single number for  $n$  is given, this is an approximation for a limited range of wavelengths (e.g., the visible range).

The absorption of light is quantified by the absorption coefficient  $\alpha$ . This is defined as the fraction of the power absorbed in a unit length of the medium, which can be expressed in Beer's law (that we have encountered several times so far) :

$$I(z) = I_0 e^{-\alpha z}.$$

The absorption coefficient is a strong function of frequency so that optical materials may absorb one color but not another.

In a similar way, scattering is described by the scattering cross section  $\sigma_s$ . Together with the number density of scatters  $N$  this leads to :

$$I(z) = I_0 e^{-N\sigma_s z}.$$

Absorption and refraction can also conveniently be described by a single quantity, the complex refractive index  $\tilde{n}$ . It is defined as  $\tilde{n} = n + ik$ , where  $n$  is the normal refractive index and  $ik$  is called the extinction coefficient (which is directly related to  $\alpha$ ).

Let us now consider the propagation of a electromagnetic wave through a medium with complex refractive index. For a plane wave travelling in  $z$  direction, the spatial and time dependence of the electric field is given by,

$$E(z, t) = E_0 e^{i(k_z z - \omega t)}$$

where  $k$  is the wave vector of the light and  $\omega$  is the angular frequency.  $E_0$  is the amplitude at  $z=0$ . In a non-absorbing medium with refractive index  $n$ , the wavelength of the light is reduced by this factor  $n$  compared to the free-space wavelength  $\lambda$ .

Therefore, we have

$$\begin{aligned} k &= \frac{2\pi}{\lambda} = n \cdot \frac{2\pi}{\lambda} = n \cdot 2\pi \cdot \frac{v}{c} \\ &= \frac{n \cdot \omega}{c} \end{aligned}$$

This can be generalized to the case of an absorbing medium by allowing the refractive index to be complex:

$$k = n \frac{\omega}{c} = (n + iK) \frac{\omega}{c}$$

Putting this in the equation for the electric field leads to:

$$\begin{aligned} E(z, t) &= E_0 e^{i(k_z z - \omega t)} \\ &= E_0 e^{i(\frac{\omega n z}{c} - \omega t)} \\ &= E_0 e^{-\frac{K \omega z}{c}} e^{i(\frac{\omega n z}{c} - \omega t)} \end{aligned}$$

(slide) This shows that a non-zero extinction coefficient leads to an exponential decay of the wave in

the medium. The intensity is proportional to the square of the amplitude of the field, namely  $I \propto E E^* = E_0^2 e^{-\frac{2Kwz}{c}}$ . Comparing this with Beer's law shows:

$$\alpha = \frac{2Kw}{c} = \frac{4\pi K}{\lambda}$$

We can relate the refractive index of a medium to its relative dielectric constant  $\epsilon_r$  by using the standard result derived from Maxwell's equations:  $n = \sqrt{\epsilon_r}$ .

Consequently, when  $n$  is complex,  $\epsilon_r$  must also be complex. We define the complex relative dielectric constant or complex dielectric function  $\tilde{\epsilon}_r = \epsilon_1 + i\epsilon_2$  and have by analogy:  $\tilde{n}^2 = \tilde{\epsilon}_r$ .

Using  $\tilde{n} = n + iK$ ,  $\tilde{\epsilon}_r = \epsilon_1 + i\epsilon_2$ , and  $\tilde{n}^2 = \tilde{\epsilon}_r^2$  we can find:

$$\begin{cases} \epsilon_1 = n^2 - K^2 \\ \epsilon_2 = 2nK \end{cases}$$

and

$$\begin{cases} n = \sqrt{\epsilon_1 + \sqrt{\epsilon_1^2 + \epsilon_2^2}} \\ K = \frac{1}{\sqrt{2}} \sqrt{-\epsilon_1 + \sqrt{\epsilon_1^2 + \epsilon_2^2}} \end{cases}$$

For weak absorption,  $K \ll n$  we have

$$n = \sqrt{\epsilon_1} \quad ; \quad K = \frac{\epsilon_2}{2n}$$

so the refractive index is mainly determined by the real part of the dielectric const., while the absorption is mainly determined by the imaginary part.

The experimental goal is then to determine  $\tilde{E}_r$  or  $\tilde{n}$  by measuring  $T$  and  $R$ . Before we take a look at the experiments, however, we will first derive a model for the propagation of light in medium.

We will treat the optically active components in the solid as dipole oscillators (Lorentz oscillator), for example an electron oscillating along its bond to the nucleus:



The frequency of such an oscillation is

Given by  $\nu_0 = \sqrt{\frac{k_s}{\mu}}$  ← spring constant

$$\text{reduced mass, } \frac{1}{\mu} = \frac{1}{m_1} + \frac{1}{m_2}$$

This dipole interacts with electromagnetic radiation: A wave can excite a dipole and consequently loose intensity, and an excited dipole can emit radiation.

The real physical nature of the dipole is not so important right now, we can think of atomic oscillators (electron vs atom), vibrational oscillators (cation vs. anion), or free electron oscillators (vibrations of the free electron gas - Drude-Lorentz model).

Now, we consider the interaction between a light wave and a dipole oscillator

with a single resonant frequency  $\omega_0$ . We model the displacement of the dipole as a damped harmonic oscillation. When we focus to the case of atomic oscillation, it is sufficient to replace the reduced mass by the mass of the electron (i.e. we ignore the motion of the nucleus). We can then write:

$$m_0 \frac{d^2x}{dt^2} + m_0 \gamma \frac{dx}{dt} + m_0 \omega_0^2 x = -e E,$$

where  $\gamma$  is the damping rate,  $e$  is the elementary charge, and  $E$  is the electric field of the light wave, which we describe by:

$$E(t) = E_0 \cos(\omega t + \phi) = E_0 \operatorname{Re}\{e^{-i(\omega t + \phi)}\}$$

The standard solution is a forced oscillation of the dipole with the frequency of the incident light:

$$x(t) = X_0 \operatorname{Re}(e^{-i(\omega t + \phi')})$$

We can get rid of the phase by allowing  $E_0$  and  $X_0$  to be complex. Putting the ansatz into the equation for the damped and forced oscillator yields:

$$X_0 = \frac{-e E_0 / m_0}{\omega_0^2 - \omega^2 - i\gamma\omega}$$

This oscillating dipole gives a resonant contribution to the macroscopic polarization (dipole moment per unit volume). If  $N$  is the number of atoms per volume,

we can write:  $\leftarrow$  dipole moment of single oscillator

$$\begin{aligned} P_{\text{res}} &= N_p \\ &= -N \chi \\ &= \frac{N^2}{\epsilon_0 m_0} \frac{\gamma}{(\omega_0^2 - \omega^2 - i\gamma\omega)} E \end{aligned}$$

Due to the form of the equation,  $P_{\text{res}}$  is small unless the frequency  $\omega$  is close to  $\omega_0$ .

Using  $D = \epsilon_0 E + P$ , we split  $P$  in the resonant and a background term:

$$\begin{aligned} D &= \epsilon_0 E + P_{\text{background}} + P_{\text{res}} \\ &= \epsilon_0 E + \epsilon_0 \chi E + P_{\text{res}} \\ &\quad \swarrow \underline{\text{electric susceptibility}} \\ &\stackrel{!}{=} \epsilon_0 \epsilon_r E \end{aligned}$$

$$\Rightarrow \boxed{\epsilon_r(\omega) = \gamma + \chi + \frac{N^2}{\epsilon_0 m_0} \frac{\gamma}{(\omega_0^2 - \omega^2 - i\gamma\omega)}}$$

This can be split into the real and the imaginary part:

$$\epsilon_r(\omega) = \gamma + \chi + \frac{N^2}{\epsilon_0 m_0} \frac{\epsilon_0^2 - \omega^2}{(\omega_0^2 - \omega^2)^2 + (\gamma\omega)^2}$$

$$\epsilon_2(\omega) = \frac{N^2}{\epsilon_0 m_0} \frac{\gamma\omega}{(\omega_0^2 - \omega^2)^2 + (\gamma\omega)^2}$$

To understand the complex dielectric function better, we first look at the low- and high-frequency limit:

$$\epsilon_r(\omega) = \epsilon_{\text{stat}} = \gamma + \chi + \frac{N^2}{\epsilon_0 m_0 \omega_0^2}$$

$$\epsilon_r(\omega) = \epsilon_\infty = \gamma + \chi$$

(72)

$$\Rightarrow (\varepsilon_{st} - \varepsilon_{\infty}) = \frac{N e^2}{\varepsilon_0 m_0 \omega_0^2}$$

Finally, we approximate for frequencies close to resonance with  $\omega \approx \omega_0 \gg \gamma$  and use

$$\Delta\omega = (\omega - \omega_0) :$$

$$\varepsilon_1(\Delta\omega) = \varepsilon_{\infty} - (\varepsilon_{st} - \varepsilon_{\infty}) \frac{2\omega_0 \Delta\omega}{4(\Delta\omega)^2 + \gamma^2}$$

$$\varepsilon_2(\Delta\omega) = (\varepsilon_{st} - \varepsilon_{\infty}) \frac{\gamma \omega_0}{4(\Delta\omega)^2 + \gamma^2}$$

These equations describe a sharp atomic absorption line centered at  $\omega_0$  with full width at half maximum equal to  $\gamma$ .

The [slide] shows the frequency dependence of  $\varepsilon_1$  and  $\varepsilon_2$  predicted by the above equations for certain values of  $\omega_0$  and  $\gamma$  as well as  $\varepsilon_{st}$  and  $\varepsilon_{\infty}$ . We see that  $\varepsilon_2$  is a strongly peaked function of  $\omega$  with a maximum value at  $\omega_0$ . The frequency dependence of  $\varepsilon_1$  is more complicated.

As we approach  $\omega_0$  from below,  $\varepsilon_1$  gradually rises from  $\varepsilon_{st}$  and reaches a peak at  $\omega_0 - \gamma/2$ . It then falls sharply, passing through a minimum at  $\omega_0 + \gamma/2$  before rising to the high-frequency limit  $\varepsilon_{\infty}$ . These line shapes are also called Lorentzian.

Also shown are the more accessible data for  $m$  and  $k$ .

In general, an optical medium will have many characteristic resonance frequencies. This can be treated in the model by just adding the contributions to  $P$  from each mode, see [slide]. Typically, atomic vibrations are in the visible and ultraviolet range, whereas vibronic excitations are in the infrared regime. We can understand this behaviour by stating at high frequencies. Here, the electrons are too slow to respond to the driving field. The medium therefore has no polarization and the dielectric constant is unity. By going down, we pass the characteristic peaks of the Lorentz oscillators with a peak in the absorption spectrum and a wiggle in the refractive index. In between the medium is transparent. The value of the refractive index in the transparent regions gradually increases as we go through more and more resonances on decreasing the frequency.

caused by the fact that  $\epsilon_{sf} > \epsilon_\infty$  which implies that  $n$  is larger below an absorption line than above it. We can compare this to experiment, e.g.  $\text{SiO}_2$  (glass), see [slide], which compares well to the simple model regarding the general features. To finish this theoretical introduction, it is important to

state that  $n(\omega)$  and  $k(\omega)$  are not independent quantities, but can be calculated from each other using the Kramers-Kronig relationships. This can be very useful in practice, because one could get the dispersion from an absorption experiment and vice versa.

Now we will turn to experiment by first discussing the measurement of absorption spectra. The easiest way to measure the absorption coefficient of a material is to make a transmission experiment on a thin platelet sample. However, as the absorption coefficient varies by several orders of magnitude according to the wavelength, this can be more difficult than it sounds. A platelet which absorbs almost nothing for a certain wavelength (too thin) may absorb almost everything for another (too thick). Usually, it is necessary to combine several techniques to determine the absorption accurately over a wide range of photon energies.

The [slide] illustrates the basic principles of transmission and reflection measurements. Light from a white-light source is filtered by a monochromator, and is incident on the sample. (See [slide] for the example of a Czerny-Turner monochromator). The transmitted and reflected light is recorded by

detectors as the photon energy is changed by scanning the monochromator. The choice of source and detector for a particular experiment depends on the spectral region in which the measurements are being made [slide]. A black body emitter such as a tungsten bulb can be used as the source for measurements in the visible or infrared spectral regions, but at higher frequencies X-ray arc lamps or other specialized UV-sources must be used. Photomultiplier tubes can be used as the detector for the visible and ultraviolet regions [slide]. For long wavelengths, semiconductor photodiodes are used. For measurements in the infrared or far in the ultraviolet, the apparatus must be enclosed within a vacuum chamber to prevent absorption by the air molecules.

The measurement mode introduced above is also called the dispersive mode. Modern spectrometers, especially for the infrared regime, use polychromatic light and deconvolute the measured signal after the sample using Fourier transformation (Fourier transform infrared spectroscopy), thereby measuring all frequencies simultaneously. (slide). The main advantages are better signal-to-noise ratio, more light intensity, and less complicated mechanics.

Another modern technique to determine the optical constants of samples is ellipsometry, the changes in polarization are measured when a light beam is reflected from or transmitted through a sample. For reflected light, this change in polarization,  $\tilde{S}$ , is often described with two values,  $\gamma$  and  $\Delta$ :

$$\tilde{S} = \tan(\gamma) e^{-i\Delta} = \frac{\tilde{R}_P}{\tilde{R}_S}$$

complex reflectivity,  
amplitude and phase

where  $\gamma$  is the ratio of the reflected amplitudes and  $\Delta$  is the phase difference produced upon reflection. Polarization changes arise from the reflectivity difference between electric field components oriented parallel ( $P$ -) and perpendicular ( $S$ -) to the plane of incidence (slide). In general, light reflection produces a change in amplitude ratio and phase difference between the  $P$ - and  $S$ -components. Ellipsometry measures this change in polarization in order to determine the sample properties. (slide)

For the case of metals and semiconductors, the optical properties are heavily influenced by the presence of free electrons. In principle, these can be treated as Lorentz oscillators with  $\omega_0 = 0$ . In the following, we will look in detail at the consequences from this model. We can treat metals (and doped semiconductors) as plasmas because they contain equal numbers of fixed positive ions and free electrons. The free electrons experience no restoring forces when they interact with electromagnetic waves. The model we will discuss here combines the Drude model of free electron conductivity with the Lorentz model of dipole oscillators, and is therefore known as the Drude - Lorentz model. In analogy to the treatment above, we write:

$$m_0 \frac{d^2x}{dt^2} + m_0 \gamma \frac{dx}{dt} = -e E_0 e^{-i\omega t}$$

where we only leave out the term for the restoring force. With the ansatz

$$x = x_0 e^{-i\omega t}$$

we obtain:

$$x = \frac{e E}{m_0 (\omega^2 + i\gamma\omega)} ,$$

and, as above:

$$\begin{aligned} D &= \epsilon_r \epsilon_0 E \\ &= \epsilon_0 E + P \\ &= \epsilon_0 E - N e x \\ &= \epsilon_0 E - \frac{N e^2 E}{m_0 (\omega^2 + i\gamma\omega)} \end{aligned}$$

Finally:

$$\epsilon_r = 1 - \frac{N_e^2}{\epsilon_0 m_0} \frac{1}{(\omega^2 + i\gamma\omega)}$$
$$= 1 - \frac{\omega_p^2}{(\omega^2 + i\gamma\omega)} \quad \text{with } \omega_p = \sqrt{\frac{N_e^2}{\epsilon_0 m_0}}$$

Plasma frequency

This is again the same result as above only with  $\omega_0 = 0$ .

For the case of weak damping ( $\gamma = 0$ ) we have:  $\epsilon_r(\omega) = 1 - \frac{\omega_p^2}{\omega^2}$

We get the reflectivity via  $\tilde{n} = \sqrt{\epsilon_r}$ .   
 $\tilde{n}$  is imaginary for  $\omega < \omega_p$  and real for  $\omega > \omega_p$ , with  $\tilde{n} = 0$  for  $\omega = \omega_p$ . The reflectivity is  $R = \left| \frac{\tilde{n}-1}{\tilde{n}+1} \right|^2$ .

For  $\omega \ll \omega_p$  we have:

$$\epsilon_r = 1 - \frac{\omega_p^2}{\omega^2} = \frac{\omega^2 - \omega_p^2}{\omega^2} \approx -\frac{\omega_p^2}{\omega^2}$$
$$\Rightarrow R = \left| \frac{-\frac{\omega_p^2}{\omega^2} - 1}{-\frac{\omega_p^2}{\omega^2} + 1} \right|^2 \approx \left| \frac{-\frac{\omega_p^2}{\omega^2}}{\frac{1}{\omega^2}} \right|^2 = 1$$

For  $\omega = \omega_p$  we have:

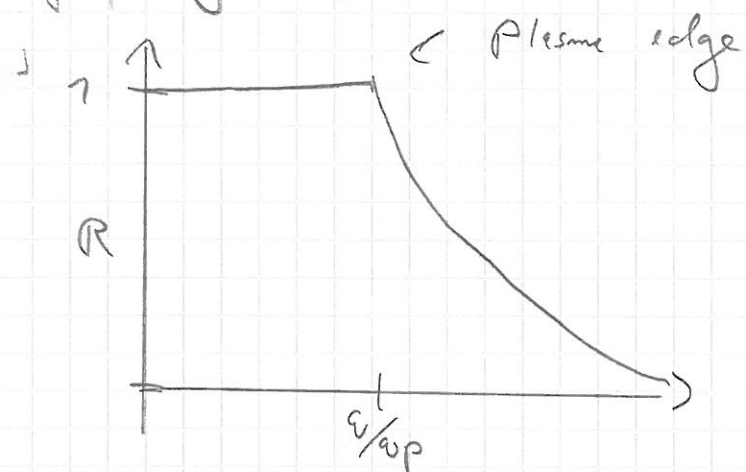
$$\epsilon_r = 1 - \frac{\omega_p^2}{\omega^2} = 0$$
$$\Rightarrow R = \left| \frac{0 - 1}{0 + 1} \right|^2 = |-1|^2 = 1$$

For  $\omega \gg \omega_p$  we have:

$$\epsilon_r = 1 - \frac{\omega_p^2}{\omega^2} = \frac{\omega^2 - \omega_p^2}{\omega^2} \approx 1$$

$$\Rightarrow R = \left| \frac{\omega - \omega_0}{\omega_0 + \omega} \right|^2 = 0$$

This frequency dependence is shown below:



A metal is thus completely reflecting up to the plasma edge. As this is usually beyond the visible part of the spectrum, metals appear shiny.